Eur. J. Biochem. **269**, 1684–1696 (2002) © FEBS 2002

Binding of *N*-acetyl-*N′*-β-D-glucopyranosyl urea and *N*-benzoyl-*N′*-β-D-glucopyranosyl urea to glycogen phosphorylase *b*

Kinetic and crystallographic studies

Nikos G. Oikonomakos[1], Magda Kosmopoulou[1], Spyros E. Zographos[1], Demetres D. Leonidas[1], Evangelia D. Chrysina[1], László Somsák[2], Veronika Nagy[2], Jean-Pierre Praly[3], Tibor Docsa[4], Béla Tóth[4] and Pál Gergely[4]

[1]*Institute of Biological Research and Biotechnology, The National Hellenic Research Foundation, Athens, Greece;*
[2]*Department of Organic Chemistry, University of Debrecen, Hungary;*
[3]*Claude-Bernard University Lyon 1, Villeurbanne, France;*
[4]*Department of Medical Chemistry, Medical and Health Science Centre, University of Debrecen, Hungary*

Two substituted ureas of β-D-glucose, *N*-acetyl-*N′*-β-D-glucopyranosyl urea (Acurea) and *N*-benzoyl-*N′*-β-D-glucopyranosyl urea (Bzurea), have been identified as inhibitors of glycogen phosphorylase, a potential target for therapeutic intervention in type 2 diabetes. To elucidate the structural basis of inhibition, we determined the structure of muscle glycogen phosphorylase *b* (GPb) complexed with the two compounds at 2.0 Å and 1.8 Å resolution, respectively. The structure of the GPb–Acurea complex reveals that the inhibitor can be accommodated in the catalytic site of T-state GPb with very little change in the tertiary structure. The glucopyranose moiety makes the standard hydrogen bonds and van der Waals contacts as observed in the GPb–glucose complex, while the acetyl urea moiety is in a favourable electrostatic environment and makes additional polar contacts with the protein. The structure of the GPb–Bzurea complex shows that Bzurea binds tightly at the catalytic site and induces substantial conformational changes in the vicinity of the catalytic site. In particular, the loop of the polypeptide chain containing residues 282–287 shifts 1.3–3.7 Å (Cα atoms) to accommodate Bzurea. Bzurea can also occupy the new allosteric site, some 33 Å from the catalytic site, which is currently the target for the design of antidiabetic drugs.

Keywords: glucopyranosyl ureas; glycogen metabolism; glycogen phosphorylase; inhibition; structure.

Glycogen phosphorylase (GP) has been exploited as a potential target for inhibitors that might prevent glycogenolysis under high glucose conditions in type 2 diabetes. Several binding sites have been identified as specific targets for inhibitor binding, and in some cases detailed X-ray crystallographic studies have elucidated key interactions responsible for inhibitor potency and have revealed the structural mechanisms of enzyme inhibition [1–9]. More specifically, the catalytic site has been probed with glucose and glucose analogue inhibitors, designed on the basis of information derived from the crystal structure of T-state glycogen phosphorylase *b* (GPb) [1–6]. The common kinetic and structural features of these compounds is that they are highly selective for GPb, they are competitive inhibitors with respect to the substrate Glc1-P, and they bind at the catalytic site by stabilizing the 280s loop (residues 282–287). In the T-state enzyme (less active), this loop partly blocks access from the surface to the buried catalytic site [10]. On transition from T state to R state (active), the 280s loop becomes disrupted and displaced, thus opening up a channel that allows substrate (glycogen) access to the catalytic site [11–16]. In the nonregulatory maltodextrin phosphorylase (MalP), the 280s loop is held permanently in an open conformation [17,18], allowing access to the catalytic site and creation of a constitutively active enzyme.

One of the early successes in the design of glucose-like compounds was the design and synthesis of *N*-acetyl-β-D-glucopyranosylamine (1-GlcNAc), which exhibited a K_i value of 32 μM, ≈60 times better than glucose (K_i = 1.7 mM) and also achieved the desired effects in modulating GP activity in hepatic cells [19,20]. The amide made a strong hydrogen bond to the main-chain carbonyl O of His377, a group for which the hydrogen-bonding capacity was otherwise unsatisfied, and the methyl group displaced two water molecules [4,5]. After crystallographic analysis of the 1-GlcNAc, a series of β-D-glucopyranosylamines were synthesized and studied in kinetic and crystallographic experiments [5], but none of them resulted in improved K_i values compared with 1-GlcNAc. The lead to

Correspondence to N. G. Oikonomakos, Institute of Biological Research and Biotechnology, The National Hellenic Research Foundation, 48 Vas. Constantinou Avenue, Athens 11635, Greece. Fax: + 3010 7273758, Tel.: + 3010 7273761, E-mail: ngo@eie.gr

Abbreviations: GP, glycogen phosphorylase; GPb, muscle glycogen phosphorylase *b*; MalP, maltodextrin phosphorylase; glucose, α-D-glucose; glucose-1-*P*, α-D-glucose 1-phosphate; Acurea, *N*-acetyl-*N′*-β-D-glucopyranosyl urea; Bzurea, *N*-benzoyl-*N′*-β-D-glucopyranosyl urea; CP320626, 5-chloro-1*H*-indole-2-carboxylic acid [1-(4-fluorobenzyl)-2-(4-hydroxypiperidin-1-yl)-2-oxoethyl]amide.

(Received 24 September 2001, revised 24 January 2002, accepted 25 January 2002)

the best glucose analogue inhibitor of GPb came from (+)-hydantocidin, a ribofuranosylidene-spiro-hydantoin; the corresponding glucopyranose derivative exhibited a K_i value of 3.1 μM, more than 500 times lower than the corresponding K_i for glucose. The compound utilized the same hydrogen bond to the CO of His377 as in 1-GlcNAc and made additional hydrogen bonds from its own CO group [3,6]. The analogous glucopyranosylidene-spiro-thiohydantoin, which can be produced in gram amounts, was recently shown to have a similar potency on GPb in the direction of glycogen breakdown (K_i = 5.1 μM) and an analogous mode of binding to GPb [21–23].

Because of its potential application to the control of hyperglycaemia in type 2 diabetes, the study of GP inhibition is a continuing challenge for physiology, synthetic, and medicinal chemistry, and also protein crystallography [8,9,24–26]. We report here on the kinetic and crystallographic studies of two new glucose derivatives, *N*-acetyl-*N*′-β-D-glucopyranosyl urea (Acurea) and *N*-benzoyl-*N*′-β-D-glucopyranosyl urea (Bzurea). Both of these compounds bind at the catalytic site. In addition, Bzurea can also occupy the so-called new allosteric inhibitor site. This compound is the first glucose analogue to show affinity for this site.

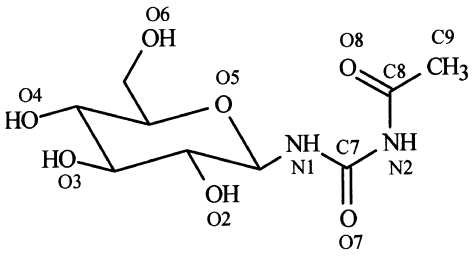

N'-acetyl-β-D-glucopyranosyl urea

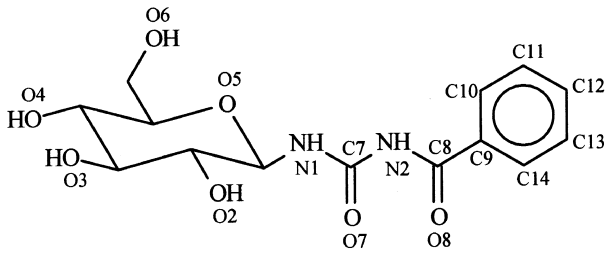

N'-Benzoyl-β-D-glucopyranosyl urea

Scheme 1. Acurea and Bzurea, showing the numbering system used.

MATERIALS AND METHODS

Rabbit GPb was isolated, purified, recrystallised four times, and assayed as described [7,8]. Glucose-1-*P* (dipotassium salt), AMP (oyster) glycogen, glucose-6-phosphate dehydrogenase, and other chemicals were obtained from Sigma Chemical Company. Glycogen was freed of AMP by the method of Helmreich & Cori [27]. Phosphoglucomutase and glucose 1,6-bisphosphate were obtained from Boehringer Mannheim GmbH.

Native T-state tetragonal ($P4_32_12$) GPb crystals were grown as previously described [28] without IMP. Before data collection, crystals were mounted in thin-walled glass capillaries and soaked with (a) 100 mM Acurea (3 h), (b) 100 mM Bzurea (1.5 h), and (c) 10 mM Bzurea (3.5 h) in a buffered solution (10 mM Bes, 0.1 mM EDTA, 0.02% sodium azide, pH 6.7). Data for GPb–Acurea complex were collected on the beamline X-31 at Hamburg (λ = 1.05 Å), at a maximum resolution of 1.97 Å. Data for the 100 mM Bzurea soak were collected on Station 9.6 at Daresbury Laboratory at a resolution of 1.80 Å (λ = 0.87 Å). Data for the 10 mM Bzurea soak were collected at a resolution of 2.26 Å on an Image Plate RAXIS IV mounted on a Rigaku Ru-H3RHB generator with a belt drive rotating anode (λ = 1.5418 Å). Crystal orientation and integration of reflections were performed using DENZO [29]. Inter-frame scaling, partial reflection summation, data reduction and postrefinement were all completed using SCALEPACK [29].

Crystallographic refinement, with either XPLOR 3.8 or CNS 1.0 using positional and individual *B*-factor refinement with bulk-solvent correction [30,31], structural analysis and comparisons were performed as previously described [7,8]. Models of Acurea and Bzurea, generated using the program SYBYL (Tripos Associates Inc., St Louis, MO, USA) were fitted to the electron-density maps after torsion angles of the computed models had been adjusted. For the bound Acurea, two possible conformations that differed by 180° in the torsion angle about N2–C8 were explored in the refinement. Both gave similar crystallographic *R* values and similar temperature factors

Table 1. Kinetic parameters for N-substituted β-D-glucopyranosylamine analogues.

Compound	Substituent at C1	K_i (μM)
N-Acetyl-*N*′-β-D-glucopyranosyl urea	β-NHCONHCOCH$_3$	370 ± 70[a]
N-Benzoyl-*N*′-β-D-glucopyranosyl urea	β-NHCONHCOPh	4.6 ± 0.9[b]
N-Acetyl-α-D-glucopyranosylamine	β-NHCOCH$_3$	32 ± 1[c]
N-Benzoyl-α-D-glucopyranosylamine	β-NHCOPh	81 ± 7[d]
N-Benzyloxycarbonyl-α-D-glucopyranosylamine	β-NHCOOCH$_2$Ph	350 ± 20[d]

[a] Calculated from double-reciprocal plots with varied Glc1-P concentrations (3–20 mM), constant concentrations of glycogen (1% w/v) and AMP (1 mM) and 0.5, 1.0, and 2.0 mM inhibitor as described in Materials and methods. [b] Calculated from double-reciprocal plots as in [a] with 10, 20, and 30 μM inhibitor. [c] Data taken from [4]. [d] Data taken from [5].

Table 2. Diffraction data and refinement statistics for GPb–Acurea and GPb–Bzurea complexes. PLP, pyridoxal 5′-phosphate.

Experiment	100 mM Acurea	100 mM Bzurea	10 mM Bzurea
Space group	$P4_32_12$	$P4_32_12$	$P4_32_12$
No. of images (degrees)	59 (0.8°)	85 (0.8°)	91 (0.8°)
Unit cell dimensions	a = b = 128.6 Å c = 116.2 Å	a = b = 128.7 Å c = 116.8 Å	a = b = 128.5 Å c = 116.5 Å
Resolution range	28.8–1.97 Å	27.84–1.80 Å	28.75–2.26 Å
No. of observations	356 285	668 695	391,254
No. of unique reflections	66 108	88 865	44 261
$< I/\sigma(I) >$ (outermost shell)[a]	16.7 (5.4)	15.63 (1.94)	10.9 (2.6)
B-values (Å^2) (Wilson plot)	17.0	25.1	28.0
Completeness (outermost shell)	95.6% (97.7%)	97.6% (95.0%)	95.8% (86.5%)
R_{merge} (outermost shell)[b]	0.048 (0.255)	0.038 (0.481)	0.096 (0.424)
outermost shell	2.00–1.97 Å	1.83–1.80 Å	2.30–2.26 Å
Multiplicity (outermost shell)	3.6 (3.4)	4.9 (4.2)	5.3 (4.2)
Refinement (resolution)	28.8–1.97 Å	27.84–1.80 Å	28.75–2.26 Å
No. of reflections used (free)	62 517 (3341 free)	84 264 (4447 free)	41 952 (2247 free)
Residues included	13–251,261–314, 325–836	13–251,261–314, 324–837	13–315,324–837
No. of protein atoms	6547	6560	6642
No. of water molecules	286	288	249
No. of ligands atoms	15 (PLP) 18 (Acurea)	15 (PLP) 46 (Bzurea)	15 (PLP) 46 (Bzurea)
Final *R* (R_{free})[c]	19.0% (21.9%)	21.5% (24.6%)	18.0% (21.3%)
R (R_{free}) (outermost shell)	23.1% (27.7%)	36.3% (37.1%)	31.4% (33.3%)
rmsd in bond lengths (Å)	0.005	0.007	0.007
rmsd in bond angles (°)	1.24	1.23	1.26
rmsd in dihedral angles (°)	22.1	24.9	25.1
rmsd in improper angles (°)	0.78	0.67	0.72
Average *B* (Å^2) for residues	13–251,261–314, 325–836	13–251,261–314, 324–837	13–315,324–837
Overall	28.7 (27.2)[d]	31.4 (29.9)[d]	33.4 (30.8)[d]
CA,C,N,O	26.5 (25.0)[d]	29.4 (27.9)[d]	31.4 (28.9)[d]
Side chain	30.8 (29.3)[d]	33.4 (31.8)[d]	35.2 (32.7)[d]
Average *B* (Å^2) for ligands			
PLP	17.5	20.1	21.2
Acurea	18.7	–	–
Bzurea (catalytic)	–	20.8	20.2
Bzurea (allosteric)	–	56.1	88.9
Water	32.8	38.9	34.6

[a] $\sigma(I)$ is the standard deviation of *I*. [b] $Rmerge = \Sigma_i \Sigma_h | < I_h > - I_{ih} | / \Sigma_i \Sigma_h I_{ih}$, where $< I_h >$ and I_{ih} are the mean and *i*th measurement of intensity for reflection *h*, respectively. [c] Crystallographic $R = \Sigma | |\boldsymbol{F}_o| - |\boldsymbol{F}_c| | / \Sigma |\boldsymbol{F}_o|$, where $|\boldsymbol{F}_o|$ and $|\boldsymbol{F}_c|$ are the observed and calculated structure factor amplitudes, respectively. R_{free} is the corresponding *R* value for a randomly chosen 5% of the reflections that were not included in the refinement. [d] Average *B* (Å^2) (given in parentheses) for protein residues if the poorly defined residues were excluded.

for the relevant atoms. However, in one conformation, the methyl group (C9) came within 2.5 Å of the N1 atom, and this unfavourable contact led us to choose the alternative conformation. A Luzatti plot [32] suggests an average positional error for all structures of ≈0.22–0.25 Å. Solvent-accessible areas were calculated with the program NACCESS [33]. Hydrogen bonds were assigned if the distance between the electronegative atoms was less than 3.3 Å and if both angles between these atoms and the preceding atoms were greater than 90°. Van der Waals interactions were assigned for nonhydrogen atoms separated by less than 4 Å. Co-ordinates for the 2.0-Å resolution GPb–Acurea, the 1.8-Å resolution GPb–Bzurea (100 mM), and the 2.26 Å resolution GPb–Bzurea (10 mM) complexes have been deposited with the RCSB Protein Data Bank (http://www.rcsb.org/) (codes 1KTI, 1K06 and 1K08, respectively).

RESULTS AND DISCUSSION

The new compounds studied in this work (Scheme 1) and their kinetic parameters (K_i) are summarized in Table 1. Crystallographic data collection, processing and refinement statistics for the structure determinations are shown in Table 2. The overall architecture of the native T-state GPb with the location of the catalytic allosteric effector and the new allosteric inhibitor site is presented in Fig. 1. Electron-density maps clearly defined the position of the inhibitors at the catalytic site (Fig. 2A,B), consistent with the kinetic results. Additional density at the new allosteric inhibitor site

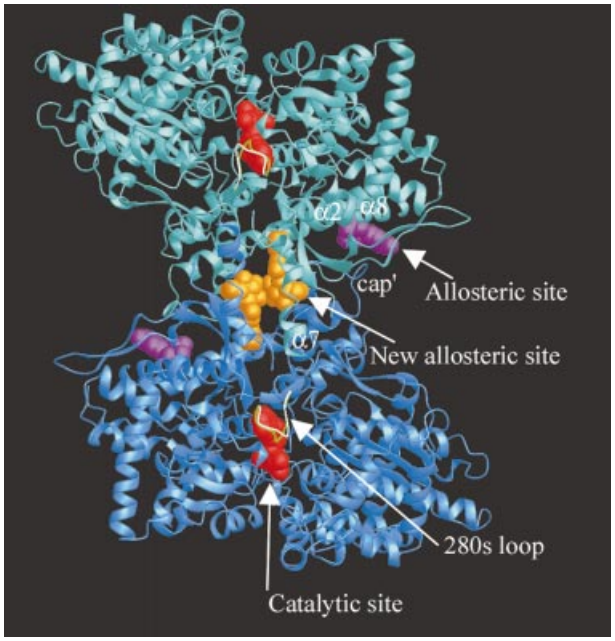

Fig. 1. A schematic diagram of the GPb dimeric molecule viewed down the twofold. The positions are shown for the catalytic, allosteric, and the new allosteric inhibitor site. The catalytic site, marked by Bzurea (shown in red), is buried at the centre of the subunit accessible to the bulk solvent through a 15-Å-long channel. By binding at this site, Bzurea promotes the less active T state through rearrangement and stabilization of the closed position of the 280s loop (shown in white and green). The allosteric site, which binds the allosteric activator AMP (shown in magenta), is situated at the subunit–subunit interface, where the C-termini of the helices α2 (residues 47–78) and α8 (residues 289–314) come together, and it is closed by the cap′ region (residues 36′ to 47′) from the symmetry-related subunit; it is some 30 Å from the catalytic site. The new allosteric inhibitor site, located inside the central cavity formed on association of the two subunits, is closed at one end by residues from the cap and α2 helices and at the other end by the tower helices (residues 262–276) and the symmetry-related residues; it binds another Bzurea molecule (shown in orange) and is some 15 Å from the allosteric effector site, 33 Å from the catalytic site, and 37 Å from the inhibitor site.

indicated binding of Bzurea (Fig. 2C) but not Acurea. We describe briefly the GPb–Acurea interactions at the catalytic site and in more detail the GPb–Bzurea interactions at both sites.

Binding of Acurea

As expected, the mode of binding of Acurea to GPb is similar to those of 1-GlcNAc, *N*-benzoyloxycarbonyl-β-D-glucopyranosylamine, and *N*-benzyloxycarbonyl-β-D-glucopyranosylamine derivatives (Table 1), but not identical. There is a hydrogen bond between the amide N atom and His377 O in the latter three analogues. In the GPb–Acurea complex, this hydrogen bond is not maintained; in the complex with Acurea, N1 is just too far away from the main-chain O of His377 (3.9 Å). However, both the carbonyl O7 and N2 contact Asp283 OD1 through a water molecule (Wat52). In addition O7 forms a hydrogen bond with the Leu136 N, and carbonyl O8 is hydrogen-bonded to the Asn284 ND2. There is also a possible intramolecular hydrogen bond from N2 to O8 as suggested by the program HBPLUS [34]. One water molecule (Wat10 in the native structure) was displaced by the methyl group (C9), in addition to those displaced by the glucopyranose (Wat284, Wat297). Acurea, on binding to GPb, makes a total of 16 hydrogen bonds and 83 van der Waals interactions (five nonpolar/nonpolar, 19 polar/polar, and 59 polar/nonpolar) (Tables 3 and 4). The hydrogen bonds formed between the ligand and the protein are illustrated in Fig. 3A.

The structural results show that Acurea can be accommodated at the catalytic site with essentially no disturbance of the structure (Fig. 4A). The rmsd between the structures of native GPb and the GPb–Acurea complex for well-defined regions (18–249, 262–312, 326–829) are 0.124, 0.134 and 0.287 Å for Cα, main-chain and side-chain atoms, respectively. By making a hydrogen bond to Asn284 and Asp283 via a water molecule and several van der Waals contacts to Asp283 OD1, Asn284 CG, OD1, and ND2 (through its O8, N2, O7, C7, and C8 atoms) Acurea stabilizes the geometry of the 280s loop. There are no changes at the allosteric effector site, the new allosteric site, the inhibitor site, or the tower/tower subunit interface.

The Acurea was found to have a K_i value of 370 μM (Table 1), indicating that it is 10 times weaker as an inhibitor than *N*-acetyl-β-D-glucopyranosylamine (K_i = 32 μM). The bound Acurea adopts a rather unfavourable conformation, formed by the intermolecular contact between its N1 and O8 (2.5 Å). Straightforward energy minimization of Acurea using the program SYBYL (with the Powell minimizer and default parameters) resulted in an extended conformation, different from the bound structure. In the bound Acurea structure, the torsion angle O7-C7-N2-C8 is 178.5°, so that the conformation about the C7–N2 bond is significantly different from that in the computed structure (0.2°) of Acurea. Although there may be some favourable energy from the release of one water molecule, the increase in conformational energy of the ligand appears to be the reason for its low binding energy.

Binding of Bzurea

Catalytic site. Bzurea binds at the catalytic site with the urea and benzoyl moieties filling the empty space of the so-called β-pocket, a side channel from the catalytic site that leads toward residue His341, but with no access to the bulk solvent [1,35]. There are in total 21 hydrogen bonds and 96 van der Waals interactions (seven nonpolar/nonpolar, 16 polar/polar, and 73 polar/nonpolar) in the GPb–Bzurea complex. There is no hydrogen bond between the amide N1 and His377 O in the Bzurea complex as in the case of the Acurea complex. N1 and N2 are hydrogen-bonded to Asp339 OD1 through two water molecules, Wat200, and Wat251 which is also hydrogen-bonded to His341 NE2 of the β-pocket (Fig. 3B). The carbonyl O7 contacts Leu136N and Gly135N and Arg569N through Wat47, and there are also water-mediated (Wat242) contacts to Gly134N and carboxyl OD1 and OD2 of Asp283, which undergoes conformational change.

There are negligible changes in the overall conformation on binding Bzurea to GPb, but there is a dramatic shift in the 280s loop with concomitant changes in the adjacent imidazole of His571, and some differences in the water

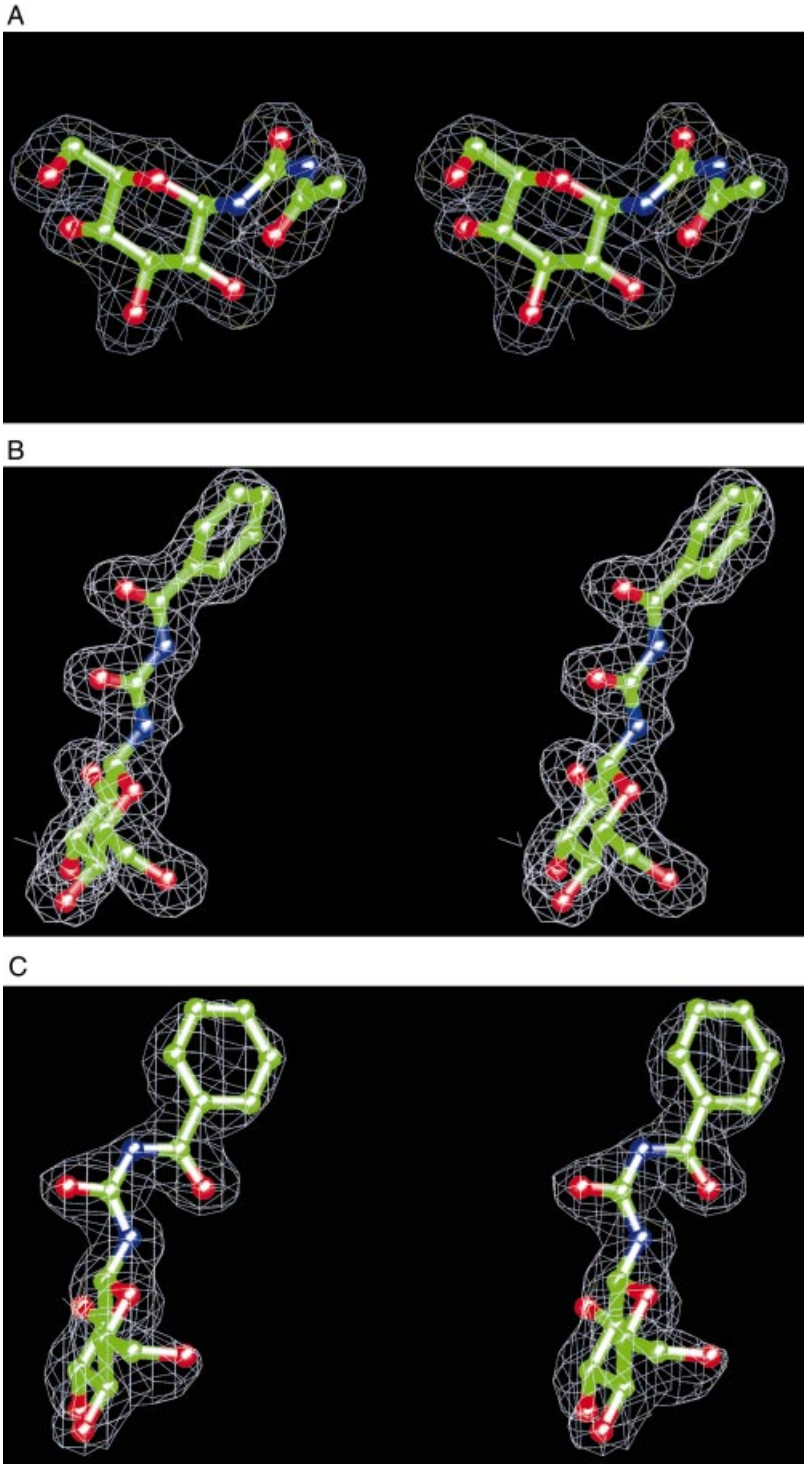

Fig. 2. Stereo diagrams of the final weighted $2F_o$-F_c electron-density maps contoured at 1σ showing the bound Acurea at the catalytic site (A), the bound Bzurea at the catalytic site (B), and the bound Bzurea at the new allosteric site (C).

structure at the catalytic site. The superimposition of the structures of the native T state GPb and the GPb–Bzurea complex over well-defined residues (18–249, 262–312, 326–829) gave rmsd of 0.253, 0.259 and 0.656 Å for Cα, main-chain and side-chain atoms, respectively, indicating that the two structures have very similar conformations. The major shifts between GPb–Bzurea and native GPb for main-chain atoms are for the residues of the 280s loop, Asn282 (1.0–1.3 Å), Asp283 (1.3–1.6 Å), Asn284 (1.3–3.7 Å), Phe285 (2.5–2.9 Å), Phe286 (1.3–1.8 Å), and Glu287 (1.4–4.1 Å) in order to optimize contacts with the ligand (Figs 3B and 4B). These conformational changes lead to increased contacts between the inhibitor and the protein. Carbonyl O8 forms a hydrogen bond to Asp283 OD1 and contacts Gly134N, Leu136N, Gly137N, and Glu88 OE2 through Wat138, while the benzoyl moiety exploits 24 van der Waals contacts in the β-pocket; these contacts are dominated by polar–polar and polar–nonpolar contacts with Asn282 and Asp283. The phenyl and His341 rings are inclined ≈ 60° and there are also two nonpolar–nonpolar contacts between

Table 3. Hydrogen bonds between Acurea and residues of the catalytic site of GPb. Wat245 is hydrogen-bonded to Lys574 NZ and Glu672 OE1 and to Gly135 N, Asp283 OD1 and Arg569 N through two other water molecules (Wat149 and Wat63, respectively); Wat101 is hydrogen-bonded to Thr671 O, Ala673 N and His377 O and to Thr378 OG1 through another water molecule (Wat218); Wat60 is hydrogen-bonded to Thr676 N and OG1; Wat52 is hydrogen-bonded to Asp283 OD1 and to Gly134 N, Gly137 N and Glu88 OE2 through another water molecule (Wat84).

Inhibitor atom	Protein atom	Distance (Å)
O2	Tyr573 OH	3.1
	Glu672 OE1	3.1
	Wat245	3.2
	Wat101	2.8
O3	Glu672 OE1	2.8
	Ser674 N	3.1
	Gly675 N	3.1
O4	Gly675 N	2.7
	Wat60	2.7
O6	His377 ND1	2.7
	Asn484 OD1	2.9
O7	Leu136 N	3.2
	Wat52	3.0
N2	Wat52	3.1
O8	Asn284 ND2	3.3

them (Tables 5 and 6). The strong affinity ($K_i = 4.6$ μM) of Bzurea for GPb can be interpreted in terms of its extensive interactions with the protein.

In the native GPb structure, His571 is hydrogen-bonded to Asp283. In the GPb–Bzurea complex, His571 is rotated ($\chi 1$) $\approx 20°$ so that ND1 and NE2 atoms are shifted 0.9 and 1.2 Å, respectively, in order to make a hydrogen bond to the new position of OD2 of Asp283. In the T state GPb, Phe285 is partially shielded by a van der Waals interaction with Tyr613, and the packing of these two aromatic groups gives rise to the nucleoside inhibitor site, a site that binds caffeine and a number of other fused ring compounds [8]. In the GPb–Bzurea complex, Asn284 is now sandwiched between the side chains of Tyr613 and Phe285 (Fig. 5B), resulting in destruction of the inhibitor site, by mimicking the T to R allosteric transition.

In fact, the key transition between inactive T-state and active R-state GP involves movement and disruption of the 280s loop, which allows a crucial arginine, Arg569, to enter the catalytic site in place of Asp283, and which also opens up access for glycogen to the catalytic site. The shift and disruption of the 280s loop is associated with subsequent destruction of the inhibitor site and changes at the intersubunit contacts of the dimer which give rise to allosteric effects [15]. In the R-state GP, the 280s loop is not well ordered and its position has not been established definitively. In contrast, in the MalP the 280s loop is held in an open conformation through interactions with the tower residues [17,18]. This allows access to the catalytic site and creates a constitutively active enzyme. Arg569 is also in the correct position to bind the substrate phosphate. A further significant conformational change in MalP structure on binding oligosaccharide (e.g. maltopentaose) involves movement of the 380 s loop (residues 377–384), resulting in closure of the catalytic site and creation of the recognition site for oligosaccharide [36].

Superimposition of MalP–G5 complex on the GPb–Bzurea complex structure over well-defined residues of the catalytic site [88 (67), 133–136 (112–115), 280–290 (256–266), 292 (268), 338–339 (306–307), 377–387 (345–355), 569 (534), 571–573 (536–538), 608 (573), 613 (578), 674–676 (639–641), 770 (737)] gave an rmsd for Cα atoms of 1.224 Å.

Table 4. Van der Waals contacts between Acurea and residues of the catalytic site of GPb.

Inhibitor atom	Protein atom	No of contacts
C1	Wat245; Leu136 N	2
C2	His377 O; Glu672 OE1; Wat245; Wat101	4
O2	His377 O; Asn284 ND2, OD1	3
C3	Glu672 OE1; Gly675 N; Wat60; Wat245	4
O3	Glu672 CG,CD; Ala673 C,CA,CB,N; Ser674 C,CA; Gly675 CA; Wat101	10
C4	Asn484 OD1; Gly675 N; Wat60	3
O4	Asn484 OD1; Ser674 C,CB; Gly675 C,CA,O; Thr676 CG2, N	8
C5	Gly135 CA, C; Leu136 N; Wat60	4
C6	Gly135 C, O; Leu136 N; His377 ND1; Asn484 OD1	5
O6	Leu139 CD2; His377 CG,CE1; Val455 CG1,CG2; Asn484 CG	6
O5	Gly135 C; Leu136 N, CA, CB; His377 CB, ND1	6
N1	Asn284 OD1; His377 O,CB	3
C7	Leu136 CB; Asn284 OD1; Wat52	3
O7	Leu136 CA, CB; Asp283 OD1; Asn284 OD1; Wat84; Wat149	6
N2	Leu136 CB; Asn284 OD1	2
C8	Asn284 ND2, OD1, CG; Asp339 OD1	4
C9	Asp339 OD1; Wat343; Wat277	3
O8	His377 C, O, CB; Asn284 OD1, CG; Thr378 CB, CG2	7
Total		83

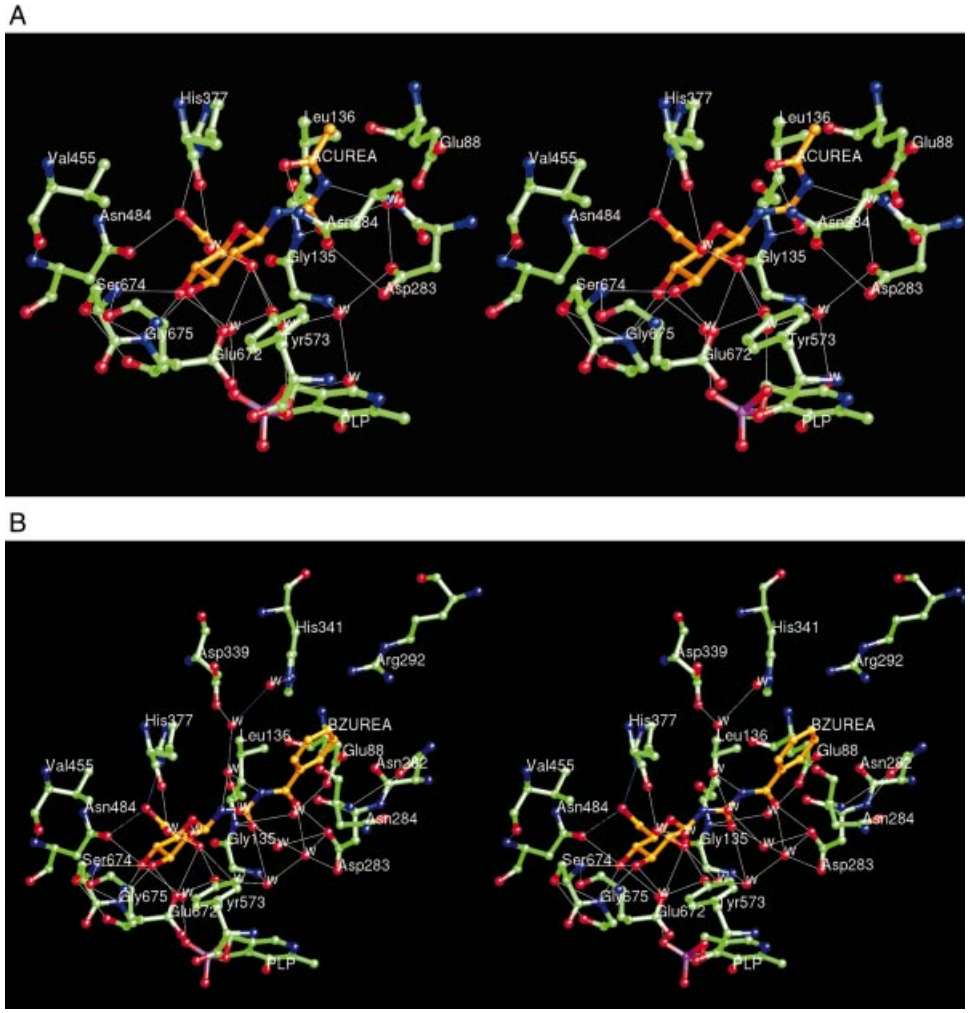

Fig. 3. Interactions between Acurea and GPb (A) and between Bzurea and GPb (B) in the vicinity of the catalytic site.

A structural comparison between GPb–Bzurea and GPb–glucose complexes and GPb–Bzurea and MalP–G5 complexes in the vicinity of the catalytic site is shown in Fig. 5B. It is apparent that the shifts in the 280s loop in the Bzurea complex are not in the direction of the T to R allosteric transition. Bzurea binds at the catalytic site by causing substantial conformational changes to the 280s loop, but the inhibitor still favours the interior position of the 280s loop because it interacts with the 280s loop. Arg569 is still in place, while there are no changes at the subunit–subunit contacts on binding Bzurea to the catalytic site. The tower helices (residues 262–276) and the cap′ (residues 36′ to 47′) α2 helix (residues 47–78) contacts in the N-terminal region of the molecule (Fig. 1) have the same positions as in the native T-state GPb. These observations indicate that Bzurea should be classified as a T-state inhibitor.

On binding Bzurea to GPb, Wat244 and Wat252 were displaced because of the shift of the 280s loop, and Wat10 and Wat201 were shifted by 1.8 Å. New water molecules, unique to the GPb–Bzurea complex structure were Wat44, Wat200, Wat242, Wat243, Wat250, Wat262 (in the position previously occupied by Asn284 OD1), and Wat268; these water molecules form important links between the ligand and the protein.

In Fig. 6, we compare the binding of 1-GlcNAc, *N*-benzyloxycarbonyl-β-D-glucopyranosylamine, *N*-benzoyl-β-D-glucopyranosylamine, Acurea, and Bzurea within the catalytic site of GPb. The positions of the glucosyl components of each of the structures are similar, indicating that the glucosyl-recognition site does not change substantially. The largest difference in positions is in their N1 positions, a difference that reflects the presence (2.9 Å in 1-GlcNAc, 3.0 Å in *N*-benzyloxycarbonyl-β-D-glucopyranosylamine, 3.2 Å in *N*-benzoyl-β-D-glucopyranosylamine) or absence (3.9 Å in Acurea and 4.2 Å in Bzurea) of a hydrogen bond between N1 and the main-chain O of His377 in these derivatives.

New allosteric inhibitor site. Bzurea, on binding to GPb, also occupies the new allosteric inhibitor site, the site that is almost buried in the central cavity of the enzyme. The new allosteric site, identified recently as a target for drug interactions [7,9], has been shown to bind a number of indole-2-carboxamide inhibitors. The conformation of the bound Bzurea is not identical with that described above for the catalytic site. In the bound Bzurea structure, the torsion angle O7-C7-N2-C8 is −179.3°, so that the conformation about the C7–N2 bond is in *trans* geometry, significantly

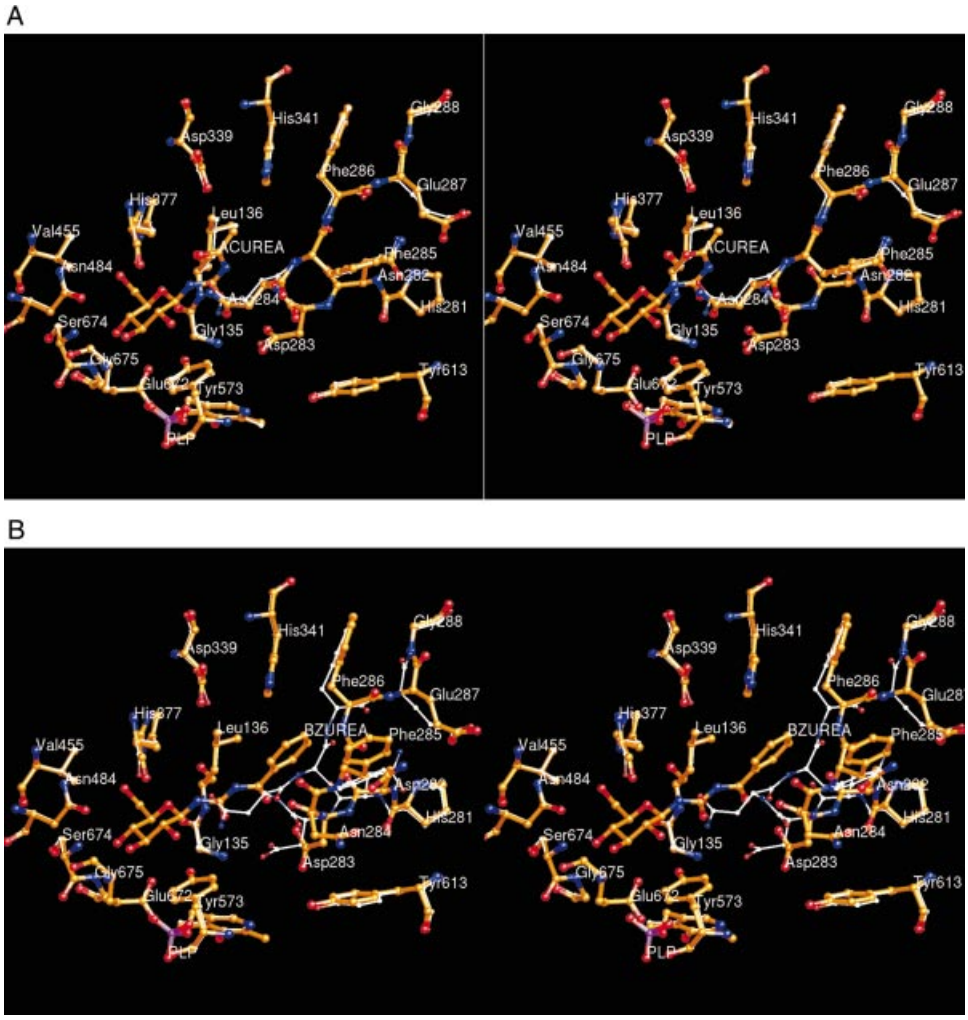

Fig. 4. Stereo diagrams showing (A) a comparison of Acurea bound to GPb (orange) with native GPb (white) in the vicinity of the catalytic site, and (B) a comparison of Bzurea (orange) bound to GPb with native GPb (white) in the vicinity of the catalytic site.

different from that in the catalytic site (0.2°) of Bzurea. In addition, the phenyl ring is coplanar to the urea moiety, whereas, at the catalytic site, the plane of the phenyl ring is inclined ≈ 30° to the plane of the urea moiety.

Bzurea on binding at the new allosteric inhibitor site of GPb makes a total of nine hydrogen bonds and exploits 80 van der Waals interactions, 28 of which are interactions between nonpolar groups; in total, there are 21 contacts with the symmetry related subunit (Fig. 7, Tables 7 and 8). The benzoyl moiety exploits 43 van der Waals contacts (25 nonpolar–nonpolar), which are dominated by the substantial contacts (20) made to almost all atoms of Arg60. There is also a hydrogen bond from the carbonyl oxygen O8 to Arg60 NH1. The urea moiety is located between the side chains of Arg60 and Lys191 and exploits 14 van der Waals contacts with residues Arg60, Glu190, Lys191, and Thr38′ (where the prime refers to residues from the symmetry-related subunit). There is a hydrogen bond from N2 to the main-chain O of Glu190, and water-mediated hydrogen bonds from carbonyl O7 to residues Asn187, Glu190, and Ala192 (Table 5). The glucopyranose moiety makes 23 van der Waals contacts, 19 of which are with residues from the symmetry-related subunit. The glucopyranose and His57′ rings are inclined ≈ 80°, and there are extensive contacts between them. There are hydrogen bonds from His57′NE2 to both hydroxy groups O3 and O4 and a rather weak hydrogen bond (3.4 Å) between hydroxyl O6 and Lys191NZ. In addition, hydroxyl groups O2 and O3 hydrogen-bond O3 and O2, respectively, of the glucopyranose from the symmetry-related bound Bzurea molecule. There is, however, only moderate complementarity of van der Waals contacts between nonpolar ligand and protein groups for this part of the molecule and there are no aromatic–aromatic, amino–aromatic and CH–π interactions that are characteristic of the tight binding of the 4-fluorobenzyl moiety of CP320626 [7].

The binding of Bzurea at the new allosteric inhibitor site of GPb does not promote extensive conformational changes except for small shifts in the atoms surrounding the inhibitor, similar to those observed on binding of CP320626 to GPb [7], i.e. of residues 60, 64, and 191, which undergo conformational changes to accommodate the ligand.

The inhibitor, on forming the complex with GPb, becomes almost entirely buried at the new allosteric site. The solvent accessibilities of the free and bound Bzurea are

Table 5. Hydrogen bonds between Bzurea and residues of the catalytic binding site of GPb. Wat81 is hydrogen-bonded to Ala N, His377 O, and Thr671 O and Thr378 OG1 through Wat232; Wat234 is hydrogen-bonded to Lys574 NZ, Tyr573 OH and Wat47; Wat47 is hydrogen-bonded to Gly135 N, Arg569 N and PLP OP3 (through Wat49), and Wat242; Wat242 is hydrogen-bonded to Gly134 N and Asp283 OD1 and OD2; Wat108 is hydrogen-bonded to Thr676 N and OG1, and PLP OP3; Wat200 is hydrogen-bonded to Wat262, and Asp339 OD1 through Wat251; Wat251 is also hydrogen-bonded to His341 NE2 and Ala383 O through Wat245; Wat138 is hydrogen-bonded to Gly134 N, Leu136 N, Gly137 N, and Glu88 OE2.

Inhibitor atom	Protein atom	Distance (Å)
O5	Leu136 N	3.3
O2	Glu672 OE1	3.1
	Tyr573 OH	3.2
	Wat81	2.8
	Wat234	2.8
O3	Gly675 N	3.1
	Ser674 N	3.1
	Glu672 OE1	2.8
O4	Gly675 N	2.7
	Asn484 OD1	3.3
	Wat108	3.0
O6	Asn484 OD1	2.8
	His377 ND1	2.7
N1	Wat200	3.0
O7	Leu136 N	3.0
	Wat47	3.3
	Wat242	3.3
N2	Wat200	2.8
O8	Wat138	2.9
	Wat242	2.8
	Asp283 OD1	3.2

525 Å^2 and 77 Å^2, indicating that a surface area of 447 Å^2 becomes inaccessible to water and that Bzurea becomes 85% buried in the enzyme complex. Binding of the inhibitor is associated with both subunits; surface areas from the two subunits that are buried in the inhibitor are 280 Å^2 (1st subunit) and 167 Å^2 (2nd subunit). Both polar and nonpolar groups are buried, but the greatest contribution comes from the nonpolar groups which contribute 306 Å^2 (84%) of the surface that becomes inaccessible. On the protein surface, a total of 162 Å^2 solvent-accessible surface area becomes inaccessible on binding Bzurea, of which 81 Å^2 (50%) is contributed by nonpolar groups. In the CP320626 (IC_{50} = 334 nM) complex [7], in contrast, the corresponding areas buried by ligand and protein are 536 Å^2 and 283 Å^2.

A structural comparison between the GPb–CP320626 complex and the GPb–Bzurea complex shows that the two proteins have very similar overall structures and do not differ significantly at the interfaces between monomers. The two structures superimpose quite well; the positions of the Cα, main-chain and side-chain atoms for residues 17–208, 212–249, 261–313, 326–549, and 558–830 deviate from their mean positions by 0.242 Å, 0.248 Å and 0.428 Å, respectively, indicating no significant changes between the complex structures. Figure 8 shows details of the contacts made at the new allosteric inhibitor site for the T-state GPb–Bzurea complex and GPb-glucose–CP320626 complex. The two structures superimpose well and they closely resemble each other in the vicinity of the new allosteric site.

In a crystallographic experiment with 10 mM Bzurea (3.5 h soak) (Table 2), electron-density maps suggested strong binding of Bzurea at the catalytic site, but partial occupancy of the new allosteric inhibitor site by the ligand. Despite the low occupancy of Bzurea, the density was sufficiently well resolved to indicate the conformation of the

Table 6. Van der Waals contacts between Bzurea and residues of the catalytic binding site of GPb.

Inhibitor atom	Protein atom	No of contacts
O5	Gly135 C; Leu136 CA,CB; His377 ND1	4
C1	Leu136 N; Wat234	2
C2	His377 O; Glu672 OE1; Wat81; Wat234	4
O2	His377 O; Wat262	2
C3	Glu672 OE1; Gly675 N; Wat108; Wat234	4
O3	Glu672 CG,CD; Ala673 N,C,CA,CB; Ser674 C,CA; Gly675 CA; Wat81	10
C4	Asn484 OD1; Gly675 N; Wat108	3
O4	Asn484 OD1; Ser674 N,C,CA,CB,OG; Gly675 O,C,CA	9
C5	Gly135 C,CA; Leu136 N; Wat108	4
C6	Gly135 C,O; Leu136 N; Leu139 CD2; His377 ND1; Asn484 OD1	6
O6	Leu139 CD2; His377 CG,CE1; Val455 CG1,CG2; Asn484 CG	6
N1	Leu136 CB; Wat262	2
C7	Leu136 N,CB; Wat200; Wat250	4
O7	Gly135 N,C,CA; Leu136 CA,CB; Wat138; Wat234	7
N2	Leu136 CB,CD1; Wat200; Wat250; Wat262	5
C8	Asp283 OD1; Wat138; Wat242	3
O8	Asn133 CB	1
C10	Asp283 O; Wat200	2
C11	Asn282 O; Asp283 O; Wat166; Wat244; Wat245	5
C12	Asn282 O; His341 CE1,NE2; Wat166; Wat244	5
C13	Glu88 OE1; Asn282 O; His341 CE1; Wat218; Wat240	5
C14	Glu88 OE1; Asn133 ND2; Wat218	3
Total		96

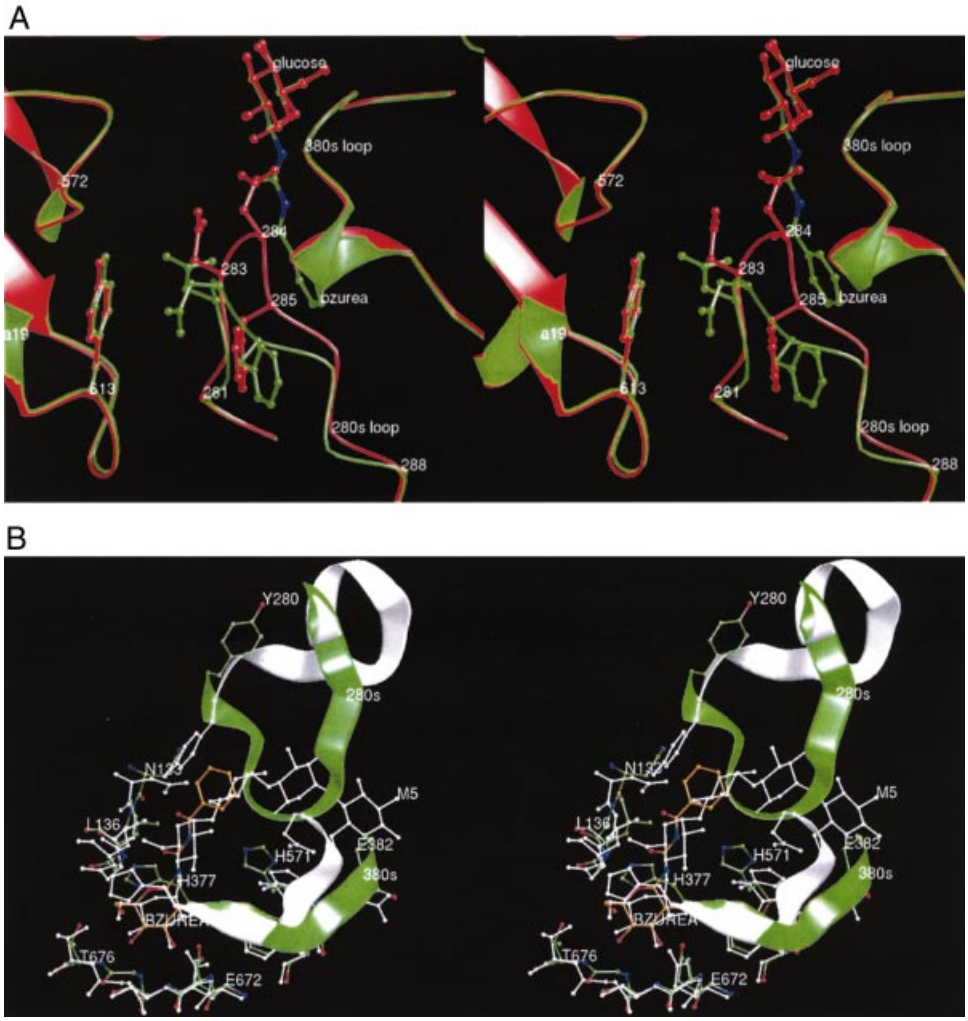

Fig. 5. Comparison between (A) the GPb–glucose complex (red) and the GPb–Bzurea complex (green) in the vicinity of the catalytic and inhibitor sites and (B) the GPb–Bzurea complex (green) and the MalP–G5 complex (white) in the vicinity of the catalytic site. (A) In the GPb–glucose complex, Phe285 from the 280s loop is stacked close to Tyr613, and, together with these two hydrophobic aromatic residues, form the inhibitor site, where caffeine (not shown) binds. (B) In the GPb–Bzurea complex, because of the substantial shift of the 280s loop, Asn284 occupies the space between Phe285 and Tyr613, thus destroying the inhibitor site. MalP and GPb have an overall 46% sequence similarity, and in the region of the catalytic site there is a 98% sequence identity [37]. In MalP the 280s loop is held in an open conformation and this allows access of G5 to the catalytic site. In contrast, in the GPb–Bzurea, the 280s loop is still in an inactive T-state conformation which blocks access to the catalytic site.

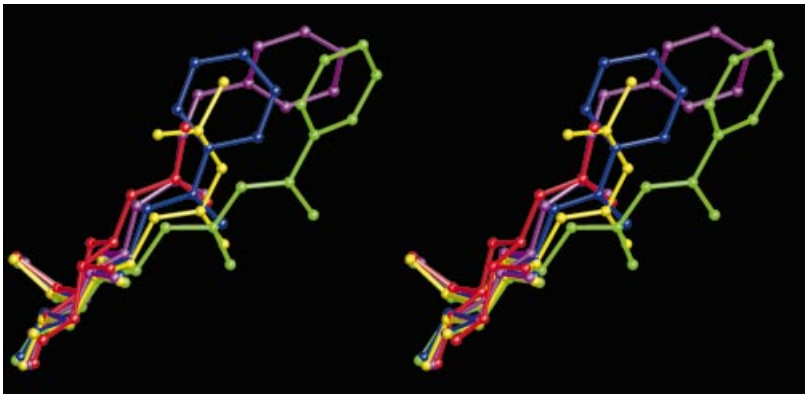

Fig. 6. Comparison of the positions of the inhibitors 1-GlcNAc (red), *N*-benzyloxycarbonyl-β-D-glucopyranosylamine (magenta), *N*-benzylacetyl-β-D-glucopyranosylamine (blue), Acurea (yellow), and Bzurea (green) bound at the catalytic site of GPb.

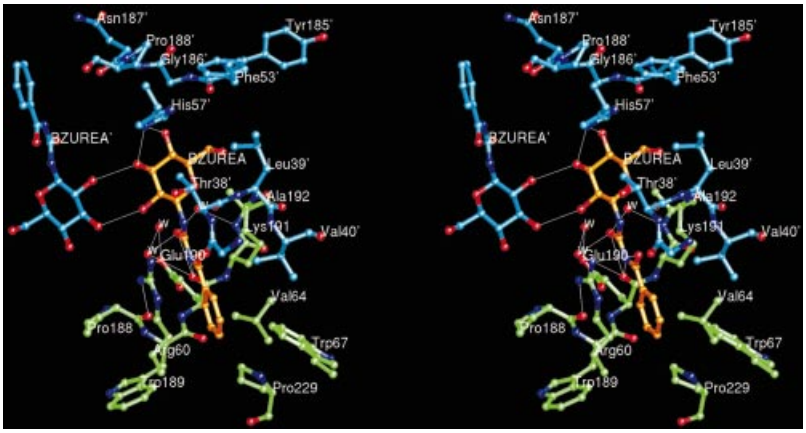

Fig. 7. Interactions between Bzurea, GPb, and water in the vicinity of the new allosteric site. Residues from subunit 1 are shown in green, and their symmetry-related equivalents (from subunit 2) are shown in cyan.

Table 7. Hydrogen bonds between Bzurea and residues of the new allosteric binding site of GPb. Wat141 is hydrogen-bonded to Ala192 N; Wat248 is hydrogen-bonded to Asn187 O, Glu190 O, Glu190 OE1 (through Wat140), and Asn187 N and Glu190 OE1 (through Wat158).

Inhibitor atom	Protein atom	Distance (Å)
O2	BZA1920 O3	3.0
O3	His57′NE2	2.9
	BZA1920 O2	3.0
O4	His57′NE2	3.3
O6	Lys191 NZ	(3.4)
O7	Wat141	2.8
	Wat248	2.8
N2	Glu190 O	2.9
O8	Arg60 NH1	3.2

ligand. It seems therefore that the new allosteric site is not the primary binding site for Bzurea.

In conclusion, this study provides high-resolution structures of GPb complexed with two substituted ureas of β-D-glucose, Acurea and Bzurea. There is a significant rearrangement of the 280s loop within the catalytic site on binding Bzurea, which is not seen in the interaction with Acurea. An additional significant feature of binding of the two ureas is the absence of a hydrogen bond to the main-chain O of His377, which is present in all substituted β-D-glucopyranosylamines studied so far. The present results indicate that Bzurea can also occupy the new allosteric inhibitor site, which is highly specific for indole-2-carboxamide inhibitors [7,9], that is currently a target for the development of hypoglycaemic drugs [26]. These observations will be of value in the design of further potent and specific inhibitors of the enzyme.

Table 8. Van der Waals contacts between Bzurea and residues of the new allosteric binding site of GPb.

Inhibitor atom	Protein atom	No of contacts
O5	Lys191 CE,NZ; Wat141; Thr38′ O	4
C1	Thr38′ O	1
C2	Thr38′ O,CG2	2
O2	Arg60 NH1; BZA1920 C3,O2	3
C3	His57′NE2; BZA1920 O2	2
O3	Thr38′ CG2; His57′ CD2,CE1,NE2	4
C4	His57′ CE1,NE2	2
O4	His57′ CE1,NE2	2
C6	Wat284′	1
O6	Leu39′ CD1; Wat284′	2
N1	Lys191 CD; Thr38′ O	2
C7	Lys191 CD; Glu190 O; Wat141; Wat248	4
O7	Glu190 O	1
N2	Arg60 CZ,NH2; Glu190 C,O; Lys191 CA,CB,CD	7
C8	Arg60 NE,CZ,NH1,NH2; Glu190 O; Lys191 CD	6
O8	Arg60 NE,CZ; Phe37′ O; Thr38′ O; Val40′ CG2	5
C9	Arg60 CD,NE,CZ	3
C10	Arg60 CG,CD,NE; Val64 CG2; Wat191; Val40′ CG2	6
C11	Arg60 CG,CD,O; Val64 CG2; Wat191	5
C12	Arg60 CG,CD; Thp67 CE3, CZ3; Pro229 CG	5
C13	Arg60 CG,CD; Trp67 CZ3; Trp189 C,O; Pro229 CD,CG	7
C14	Arg60 CD; Pro188 O; Trp189 C,O; Glu190 C,O	6
Total		80

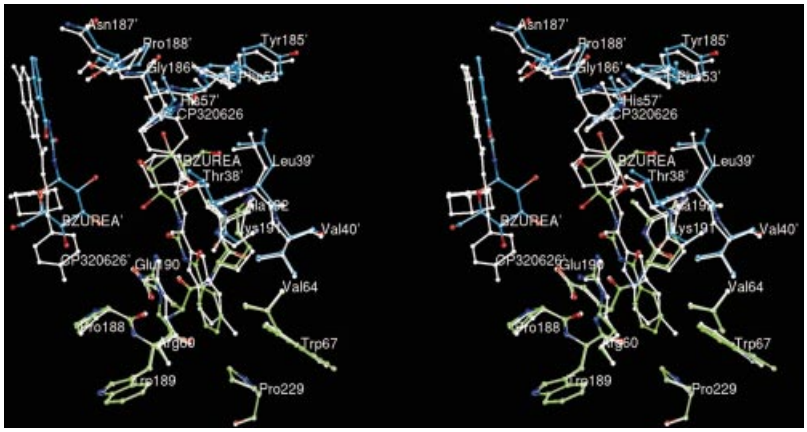

Fig. 8. Stereo diagram showing a comparison of Bzurea bound to GPb with CP320626 bound to GPb in the vicinity of the new allosteric site. Green: GPb–Bzurea complex (subunit 1); cyan: GPb–Bzurea complex (subunit 2); white: GPb–glucose–CP320626 complex. All figures were produced using XOBJECTS (M. E. M. Noble, Laboratory of Molecular Biophysics, University of Oxford, UK, unpublished results).

ACKNOWLEDGEMENTS

This work was supported by the Greek GSRT (PENED1999, 99ED237), the Joint Research and Technology project between Greece and Hungary (2000–2002) (to N. G. O. and P. G.), the Hungarian Academy of Sciences and CNRS, France supporting the collaboration of L. S. and J. P. P., the Hungarian Ministry of Education (FKFP 423/2000), the Hungarian Ministry of Health (ETT 01/2000), the Zsigmond Diabetes Foundation (Hungary), the EMBL Hamburg Outstation through the IHPP (HPRI-CT-1999-00017), and the SRS Daresbury Laboratory through the (IHPP HPRI-CT-1999-00012).

REFERENCES

1. Martin, J.L., Veluraja, K., Johnson, L.N., Fleet, G.W.J., Ramsden, N.G., Bruce, I., Oikonomakos, N.G., Papageorgiou, A.C., Leonidas, D.D. & Tsitoura, H.S. (1991) Glucose analogue inhibitors of glycogen phosphorylase: the design of potential drugs for diabetes. *Biochemistry* **30**, 10101–10116.
2. Watson, K.A., Mitchell, E.P., Johnson, L.N., Son, J.C., Bichard, C.J.F., Orchard, M.G., Fleet, G.W.J., Oikonomakos, N.G., Leonidas, D.D., Kontou, M. & Papageorgiou, A.C. (1994) Design of inhibitors of glycogen phosphorylase: a study of α- and β-C-glucosides and 1-thio-β-D-glucose compounds. *Biochemistry* **33**, 5745–5758.
3. Bichard, C.J.F., Mitchell, E.P., Wormald, M.R., Watson, K.A., Johnson, L.N., Zographos, S.E., Koutra, D.D., Oikonomakos, N.G. & Fleet, G.W.J. (1995) Potent inhibition of glycogen phosphorylase by a spirohydantoin of glucopyranose: first pyranose analogues of hydantocidin. *Tetrahedron Letts.* **36**, 2145–2148.
4. Oikonomakos, N.G., Kontou, M., Zographos, S.E., Watson, K.A., Johnson, L.N., Bichard, C.J.F., Fleet, G.W.J. & Acharya, K.R. (1995) N-acetyl-α-D-glucopyranosylamine: a potent T state inhibitor of glycogen phosphorylase. A comparison with β-D-glucose. *Protein Sci.* **4**, 2469–2477.
5. Watson, K.A., Mitchell, E.P., Johnson, L.N., Cruciani, G., Son, J.C., Bichard, C.J.F., Fleet, G.W.J., Oikonomakos, N.G., Kontou, M. & Zographos, S.E. (1995) Glucose analogue inhibitors of glycogen phosphorylase: from crystallographic analysis to drug prediction using GRID force-field and GOLPE variable selection. *Acta Crystallogr.* **D51**, 458–472.
6. Gregoriou, M., Noble, M.E.M., Watson, K.A., Garman, E.F., Krulle, T.M., Fuente, C., Fleet, G.W.J., Oikonomakos, N.G. & Johnson, L.N. (1998) The structure of a glycogen phosphorylase glucopyranose spirohydantoin complex at 1.8 Å resolution and 100 K: the role of the water structure and its contribution to binding. *Protein Sci.* **7**, 915–927.
7. Oikonomakos, N.G., Skamnaki, V.T., Tsitsanou, K.E., Gavalas, N.G. & Johnson, L.N. (2000) A new allosteric site in glycogen phosphorylase *b* as a target for drug interactions. *Structure* **8**, 575–584.
8. Oikonomakos, N.G., Zographos, S.E., Skamnaki, V.T., Tsitsanou, K.E. & Johnson, L.N. (2000) Flavopiridol inhibits glycogen phosphorylase by binding at the inhibitor site. *J. Biol. Chem.* **275**, 34566–34573.
9. Rath, V.L., Ammirati, M., Danley, D.E., Ekstrom, J.L., Gibbs, E.M., Hynes, T.R., Mathiowetz, A.M., McPherson, R.K., Olson, T.V., Treadway, J.L. & Hoover, D.J. (2000) Human liver glycogen phosphorylase inhibitors bind at a new allosteric site. *Chem. Biol.* **7**, 677–682.
10. Johnson, L.N., Hajdu, J., Acharya, K.R., Stuart, D.I., McLaughlin, P.J., Oikonomakos, N.G. & Barford, D. (1989) Glycogen phosphorylase *b*. In *Allosteric Enzymes* (Herve, G., ed.), pp. 81–127. CRC Press, Boca Raton, FL.
11. Sprang, S.R., Acharya, K.R., Goldsmith, E.J., Stuart, D.I., Varvill, K., Fletterick, R.J., Madsen, N.B. & Johnson, L.N. (1988) Structural changes in glycogen phosphorylase induced by phosphorylation. *Nature (London)* **336**, 215–221.
12. Barford, D. & Johnson, L.N. (1989) The allosteric transition of glycogen phosphorylase. *Nature (London)* **340**, 609–616.
13. Barford, D., Hu, S.H. & Johnson, L.N. (1991) Structural mechanism for glycogen phosphorylase control by phosphorylation and AMP. *J. Mol. Biol.* **218**, 233–260.
14. Sprang, S.R., Withers, S.G., Goldsmith, E.J., Fletterick, R.J. & Madsen, N.B. (1991) Structural basis for activation of glycogen phosphorylase *b* by adenosine monophosphate. *Science* **254**, 1367–1371.
15. Johnson, L.N. (1992) Glycogen phosphorylase: control by phosphorylation and allosteric effectors. *FASEB J.* **6**, 2274–2282.
16. Oikonomakos, N.G., Acharya, K.R. & Johnson, L.N. (1992) Rabbit muscle glycogen phosphorylase b: structural basis of activation and atalysis. In *Post-Translational Modification of Proteins* (Harding, J.J. & Crabbe, M.J.C., eds), pp. 81–151. CRC Press, Boca Raton, FL, USA.
17. O'Reilly, M., Watson, K.A., Schinzel, R., Palm, D. & Johnson, L.N. (1997) Oligosaccharide substrate binding in *Escherichia coli* maltodextrin phosphorylase. *Nat. Struct. Biol.* **4**, 405–412.
18. Watson, K.A., Schinzel, R., Palm, D. & Johnson, L.N. (1997) The crystal structure of *Escherichia coli* maltodextrin phosphorylase provides an explanation for the activity without control in this basic archetype of a phosphorylase. *EMBO J.* **16**, 1–14.
19. Board, M., Hadwen, M. & Johnson, L.N. (1995) Effects of novel analogues of D-glucose on glycogen phosphorylase activies in crude extracts of liver and skeletal muscle. *Eur. J. Biochem.* **228**, 753–761.

20. Board, M., Bollen, M., Stalmans, W., Kim, Y., Fleet, G.W.J. & Johnson, L.N. (1995) Effects on a C1 substituted glucose analogue on the activation states of glycogen synthase and glycogen phosphorylase in rat hepatocytes. *Biochem. J.* **311**, 845–852.
21. Ösz, E., Somsák, L., Szilágyi, L., Kovács, L., Docsa, T., Tóth, B. & Gergely, P. (1999) Efficient inhibition of muscle and liver glycogen phosphorylases by a new glucopyranosylidene-spiro-thiohydantoin. *Bioorg. Med. Chem. Lett.* **9**, 1385–1390.
22. Somsák, L., Nagy, V., Docsa, T., Tóth, B. & Gergely, P. (2000) Gram-scale synthesis of a glucopyranoslidene-spyro-thiohydantoin and its effect on hepatic glycogen metabolism studied *in vitro* and *in vivo*. *Tetrahedron: Asym.* **11**, 409–412.
23. Oikonomakos, N.G., Skamnaki, V.T., Ösz, E., Szilágyi, L., Somsák, L., Docsa, T., Tóth, B. & Gergely, P. (2001) Kinetic and crystallographic studies of glucopyranosylidene spiro-thiohydantoin binding to glycogen phosphorylase *b*. *Bioorg. Med. Chem.* **10**, 261–268.
24. Ainston, S., Hampson, L., Gomez-Foix, A.M., Guinovart, J.J. & Agius, L. (2001) Hepatic glycogen synthesis is highly sensitive to phosphorylase activity: evidence from metabolic control analysis. *J. Biol. Chem.* **276**, 23858–23866.
25. Somsák, L., Kovács, L., Tóth, M., Ösz, E., Szilágyi, L., Györgydeák, Z., Dinya, Z., Docsa, T., Tóth, B. & Gergely, P. (2001) Synthesis of and a comparative study on the inhibition of muscle and liver glycogen phosphorylases by epimeric pairs of D-gluco- and D-xylopyranosylidene-spiro-(thio)hydantoins and *N*-(D-glucopyaranosyl) amides. *J. Med. Chem.* **44**, 2843–2848.
26. Treadway, J.L., Mendys, P. & Hoover, D.J. (2001) Glycogen phosphorylase inhibitors for tratment of type 2 diabetes mellitus. *Exp. Opin. Invest. Drugs* **10**, 439–454.
27. Helmreich, E.J.M. & Cori, C.F. (1964) The role of adenylic acid in the activity of phosphorylase. *Proc. Natl Acad. Sci. USA* **51**, 131–138.
28. Oikonomakos, N.G., Melpidou, A.E. & Johnson, L.N. (1985) Crystallisation of pig skeletal phosphorylase b. Purification, physical and catalytic characterization. *Biochim. Biophys. Acta* **832**, 248–256.
29. Otwinowski, Z. & Minor, W. (1997) Processing of x-ray diffraction data collected in oscillation mode. *Methods Enzymol.* **276**, 307–326.
30. Brunger, A.T. (1992) X-PLOR, Version 3.1. *A System for X-Ray Crystallography and NMR*. Yale University Press, New Haven, CT, USA.
31. Brunger, A.T., Adams, P.D., Clore, G.M., DeLano, W.L., Gros, P., Grosse-Kunstleve, R.W., Jiang, J.-S., Kuszewski, J., Nilges, M., Pannu, N.S., Read, R.J., Rice, L.M., Simonson, T. & Warren, G.L. (1998) Crystallography and NMR system; A new software suite for macromolecular structure determination. *Acta Crystallogr.* **D54**, 905–921.
32. Luzatti, V. (1952) Traitement statistique des erreurs dans la determination des structure crystallines. *Acta Crystallogr.* **5**, 802–810.
33. Hubbard, S.J. & Thornton, J.M. (1993) *NACCESS, Computer Program*. Department of Biochemistry and Molecular Biology, University College London, London, UK.
34. McDonald, I.K. & Thornton, J.M. (1994) Satisfying hydrogen bonding potential in proteins. *J. Mol. Biol.* **238**, 777–793.
35. Barford, D., Schwabe, J.W.R., Oikonomakos, N.G., Acharya, K.R., Hajdu, J., Papageorgiou, A.C., Martin, J.L., Knott, J.C.A., Vasella, A. & Johnson, L.N. (1988) Channels at the catalytic site of glycogen phosphorylase *b*: binding and kinetic studies with the β-glycosidase inhibitor D-gluconohydroximo-1,5-lactone *N*-phenylurethane. *Biochemistry* **27**, 6733–6741.
36. Watson, K.A., McCleverty, C., Geremia, S., Cottaz, S., Driguez, H. & Johnson, L.N. (1999) Phosphorylase recognition and phosphorolysis of its oligosaccharide substrate: answers to a long outstanding question. *EMBO J.* **17**, 4619–4632.
37. Palm, D., Goerl, R. & Burger, K.J. (1985) Evolution of catalytic and regulatory sites in phosphorylase. *Nature (London)* **313**, 500–502.